Study on the Performance Evaluation of Heliostat Field Based on Multiple Ray Tracing Method

Hongyan Gao [#,*], Junjie Zou [#], Denghui Yang, Xinqi Wang

School of Semiconductors and Physics, North University of China, Taiyuan, China, 030051

* Corresponding Author Email: 13781790790@163.com

[#]These authors contributed equally.

Abstract. Environmental pollution and the energy crisis are two significant obstacles impeding the sustainable development of human society today. Tower solar thermal power generation emerges as a promising low-carbon and environmentally friendly clean energy technology. Consequently, the meticulous evaluation of the performance of the fixed-sun mirror field in tower solar thermal power generation is paramount in optimizing its output power. Taking the example of the 100 MW molten salt tower solar thermal power station in Gansu Dunhuang City Photovoltaic Industrial Park, this paper delves into its performance research. Since the sun's rays cannot uniformly reach the collector tower, an analysis based on the angle of incidence reveals an annual average cosine efficiency of 0.7565. Moreover, shading losses due to reflections between heliostat mirrors can occur. To address this, the paper employs the multi-ray tracing method to ascertain the shading loss rate, arriving at an annual average shading efficiency of 0.8268. Additionally, the reflected light, even without shading, may fail to reach the collector, resulting in truncation losses. The energy flow density method is adopted to determine an annual average truncation efficiency of 0.7418. Other factors, such as an air transmittance rate of 0.9652 and a specular reflectance rate of 0.92, contribute to an overall annual average optical efficiency of 0.4134. With these efficiencies in mind, the annual average thermal power output of the mirror field is calculated to be 25.13 MW. The number and area of heliostat mirrors jointly determine the total lighting area, and calculations reveal that the annual average thermal power output per unit area of mirrors stands at 0.4001 kW/m2. This comprehensive analysis offers crucial insights into the performance optimization of tower solar thermal power generation systems, paving the way for a more sustainable energy future.

Keywords: New Clean Energy, Multiple Ray Tracing Method, Energy Flow Density Method, Optical Efficiency.

1. Introduction

Tower solar thermal power generation usually uses a large number of heliostats to emit solar thermal radiation to the high-temperature heat absorber at the top part of the heat-absorbing tower using a concentrating subsystem [1]. And the heliostat is the concentrating device in the tower solar thermal power generation system, which mainly consists of optical mirrors, support structure, columns, transmission system and tracking control system. Azimuth-pitch tracking is the most widely used two-axis tracking method of heliostat [2]. The horizontal axis is equipped with planar mirrors and the azimuth and pitch angles of the mirrors are controlled by the longitudinal axis and the horizontal axis, respectively. Liu Jiaying et al [3]. proposed a dual-axis tracking method based on heliostat orbit tracking and "altitude-azimuth" to realize the tracking of the sun. Wei Xiudong [4] and others used Monte Carlo ray tracing method to establish the mathematical model of mirror field concentrating light. All the above studies analyze the optimization of the layout of the heliostat mirror field of the tower solar energy, but fewer scholars have evaluated the performance of the heliostat mirror field at present.

Based on this research background, this paper establishes a mathematical model with reference to a 100 MW-scale molten salt tower-type photovoltaic power plant in Dunhuang, Gansu to evaluate the performance of its heliostat mirror field. The multiple ray tracing method is used to determine the shading loss rate[5], and the energy flow density method is used to obtain the annual average truncation efficiency, air transmittance, and specular reflectance, which in turn yields the annual

average optical efficiency[6], and ultimately the annual average output thermal power of the heliostat mirror field.The annual average thermal power output of the heliostat mirror field is 0.4001KW/m2, compared with the actual annual average thermal power output of 0. 44KW/m2 of the heliostat mirror field.

2. Background knowledge of the performance of the heliostat field

(1) Mirror reflectivity: the combined efficiency of the reflectivity of the mirror and the degree of mirror tarnish.

(2) Cosine Loss: A reduction in received energy due to the direction of solar incidence not being parallel to the direction normal to the mirror light pickup opening.

(3) Atmospheric attenuation loss: sunlight in the air propagation process, due to atmospheric gases, dust, etc. on the light caused by a certain degree of attenuation, so the light path from the mirror reflected to the collector, due to the distance between the mirror and the target reflective point of the loss of its also different.

(4) Shadow blocking loss: When irradiated by the sun, there are light-facing and backlight-facing surfaces of mirrors. In the fixed-sun mirror field in the shadow of the fixed-sun mirror in another fixed-sun mirror to meet the range, or reflected light reflected to the back of the other fixed-sun mirror and other similar situations caused by the mirror field to receive the light attenuation, resulting in a shadow shading loss.

(5) truncation loss: when the mirror field reflection of a wide range of collector acceptance surface range, by the characteristics of the spot and the precision of the fixed-sun mirror or shaking may cause spot shift and other situations, thus making part of the light fall into the collector outside, these overflow spot caused by the overflow loss.

(6) solar altitude angle α_s: the angle between the sun's rays at a certain place and the surface cut surface connected to the earth's center through the place, which is calculated by the formula $\sin\alpha_s = \cos\delta\cos\varphi\cos\omega + \sin\delta\sin\varphi$, of which δ is the sun's angle of declination, φ is the local latitude, and ω is the sun's angle of time.

(7) Solar azimuth γ_s: The angle measured in the clockwise direction with the north direction of the target as the starting direction and the incidence direction of the sunlight as the termination direction, which is calculated by the formula $\cos\gamma_s = \dfrac{\sin\delta - \sin\alpha_s\sin\varphi}{\cos\alpha_s\cos\varphi}$.

(8) Solar declination angle δ [7]: the angle of intersection of the Earth's rotational orbital plane and the equatorial plane, which is calculated as $\sin\delta = \sin\dfrac{2\pi D}{365}\cdot\sin\left(\dfrac{2\pi}{360}\cdot 23.45\right)$, where D is the number of days counted from the vernal equinox as the 0th day.

(9) solar time angle ω: from the observation point celestial sphere meridian circle along the celestial equator amount to the sun where the angular distance of the time circle, the formula for its $\omega = \dfrac{\pi}{12}\cdot(ST-12)$, where ST for the local time.

From the above definition, it can be seen that, for any location on the earth, the angle of solar declination is 0° at the vernal or autumnal equinox, and the azimuth of the sun at sunrise is 90°. At the same time, the sun rises at different angles of solar declination, when it is greater than 0°, the sun rises from the north-east direction; less than 0 °, the sun rises from the south-east direction. In addition, the angle of declination also affects the size of the angle of direction of sunset.

(10) Establishment of a coordinate system for the heliostat field

The coordinate system for establishing a fixed-heaven mirror field is shown in Fig 1.

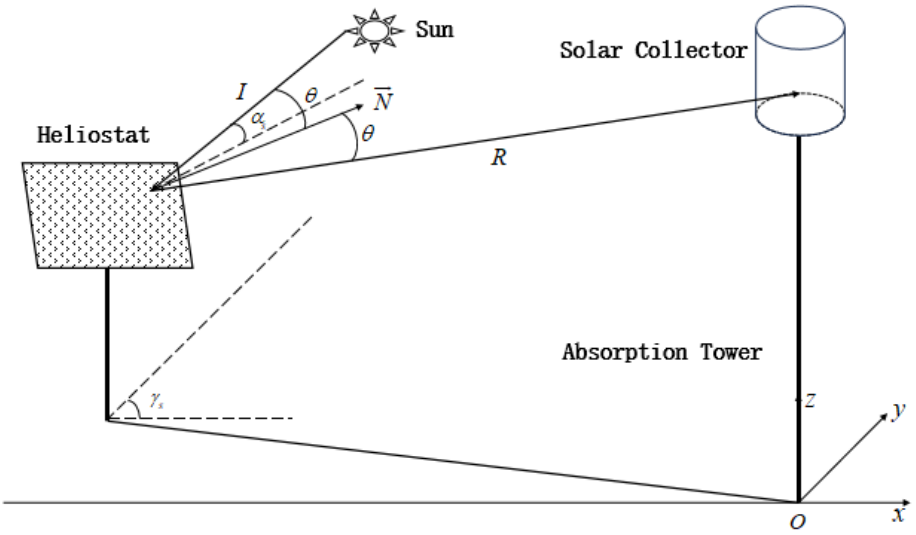

Figure 1. Schematic of the coordinate system of the heliostat field

In Fig 2, the east direction is the positive direction of x , the north direction is the positive direction of y , and the upward direction of the absorber tower is the positive direction of z . Among them, I is the sun's incident ray, R is the sun's reflected ray, $\vec{N}$ is the normal vector of the mirror surface of the heliostat, θ is the angle of incidence (or reflection), α_s is the sun's altitude angle, γ_s is the sun's azimuth angle.

(11) Establishment of mirror coordinate system

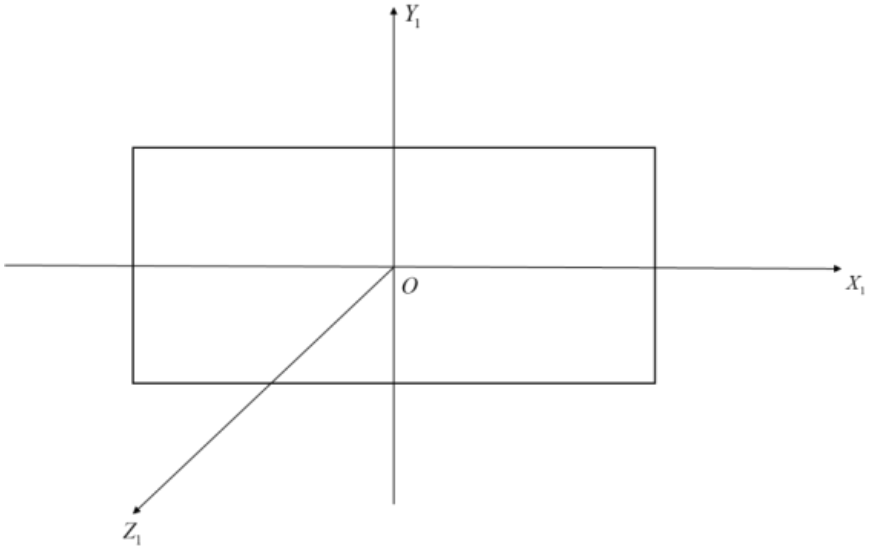

Figure 2. Mirror coordinate system

In Fig. 2, due east is the x axis positive direction, due north is the y axis positive direction, and the vertical direction of the ground up is the z axis positive direction.

3. Optical efficiency determined by multiple loss factors

3.1. Cosine efficiency

When the sun's rays are incident perpendicular to the plane, the fixed-sun mirror receives the highest amount of energy. However, there is a cosine loss when the sun's rays are at an angle to the plane, so there is also a cosine loss when the sunlight is incident on the heliostat. The schematic diagram is shown in Fig3.

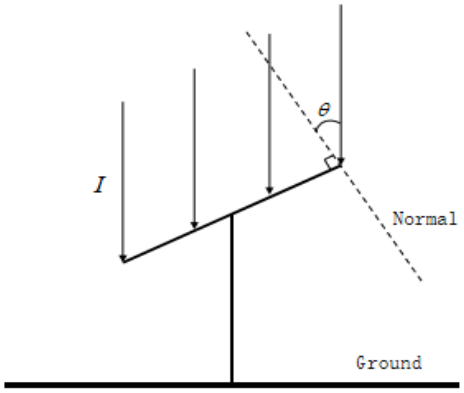

Figure 3. Schematic diagram of cosine efficiency

Based on the position of the sun, the solar incident light is calculated and its direction vector expression is given in equation (1).

$$\vec{I}=\left(\cos\alpha_s\cdot\cos\gamma_s,\cos\alpha_s\cdot\sin\gamma_s,\sin\alpha_s\right), \tag{1}$$

Where α_s is the sun's altitude angle, γ_s is the sun's azimuth angle, and the vector $\vec{I}$ is oriented with the center of the mirror pointing toward the sun.

The collector works by collecting the reflected light from the heliostats in all directions, so the reflected light from all heliostats points to the center of the collector, represented by the center of the heliostat. Known coordinates of the center of each fixed-sun mirror and the coordinates of the center of the collector, according to the principle of the two points to determine a straight line and then find the reflected light from each fixed-sun mirror, the direction of the reflected light vector expression as in equation (2).

$$\vec{R}=\left(\frac{-x}{\sqrt{x^2+y^2+H^2}},\frac{-y}{\sqrt{x^2+y^2+H^2}},\frac{h}{\sqrt{x^2+y^2+H^2}}\right), \tag{2}$$

Where, h is the height of the fixed-sun mirror and the tower base height of the absorber tower, H is the height of the absorber tower, and the vector $\vec{R}$ is directed from the center of the collector to the center of the mirror.

The expression for the angle of incidence θ is given in equation (3).

$$\theta=\frac{1}{2}\arccos\left(-\vec{I}\cdot\vec{R}^T\right), \tag{3}$$

Therefore, the cosine efficiency [5] is shown in equation (4).

$$\eta_{\cos}=1-\text{Cosine loss}=\cos\theta=\frac{1}{2}\left(-\vec{I}\cdot\vec{R}^T\right), \tag{4}$$

The average of the different moments of the 21st day of each month is taken as the monthly average cosine efficiency for that month and the data is obtained with the help of MATLAB as shown in Table 1.

Table 1 Average cosine efficiency at 21 days per month

Date	Average cosine efficiency	Date	Average cosine efficiency
1.21	0.7199	7.21	0.7892
2.21	0.7404	8.21	0.7786
3.21	0.7611	9.21	0.7601
4.21	0.7793	10.21	0.7378
5.21	0.7893	11.21	0.7182
6.21	0.7924	12.21	0.7111

3.2. Atmospheric transmittance

The expression for atmospheric transmittance is shown in equation (5).

$$\eta_{at} = 0.99321 - 0.0001176 d_{HR} + 1.97 \times 10^{-8} \times d_{HR}^2 \tag{5}$$

Where d_{HR} is the distance from the center of the mirror to the center of the collector and $d_{HR} \leq 1000$.

3.3. Shadow Occlusion Efficiency

In heliostat emission, shadow shading loss caused by shadow shading is to be avoided, which depends on the distance between each heliostat, and its effect is negligible when the distance is too large. In addition, the shadow shading loss is closely related to the mirror discharge, but also inseparable from the operation of the sun[8]. If the sun's altitude angle is very large, such as noon, the summer solstice, neighboring heliostats produce less shadow blocking loss; on the contrary, if the sun's altitude angle is small, such as early morning, dusk time, the neighboring heliostats between the shadow blocking loss is larger.

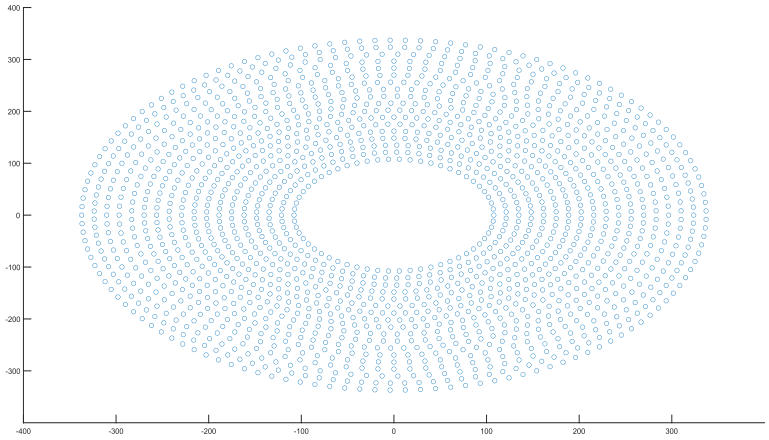

Figure 4 Schematic distribution of heliostats

Combined with Fig. 4, it is found that the distribution of heliostats has symmetry, and the direction of sunrise is first biased toward the side of the mirror field, so this paper selects the eight groups of neighboring heliostat coordinates with symmetrical inner and outer circles as representative as shown in Table 2.

Table 2 Eight groups represent heliostat coordinates

Section	Coordinate		Section	Coordinate	
1	$(107.882,0)$	$(107.25,11.664)$	5	$(-337.132,0)$	$(-336.732,-16.414)$
2	$(107.882,0)$	$(107.25,-11.664)$	6	$(-337.132,0)$	$(-336.732,16.414)$
3	$(-107.882,0)$	$(-107.25,11.664)$	7	$(323.275,0)$	$(323.275,-15.517)$
4	$(-107.882,0)$	$(-107.25,-11.664)$	8	$(337.032,-8.210)$	$(337.032,8.210)$

There are two situations that cause energy loss during the convergence of light in tower solar thermoelectric systems: shadows and occlusion. Shadow represents the ineffective area caused by light being obstructed by the surrounding heliostat and unable to reach the target heliostat, while occlusion represents the ineffective area caused by light being obstructed by the surrounding heliostat during the reflection from the target heliostat to the receiver [9]. With the help of MATLAB calculations to get each time point of the collector tower shadow and the intersection of this mirror

field is less, so this paper is ignored; for the incident light blocking this paper assumes that all can be incident, the number of intersections of reflected light and blocking mirrors has been included, so this paper only considers two mirrors to reflect the light whether the light is blocked in this case.

Calculate the shadow occlusion loss realistically to calculate whether any point on the mirror M_1 falls within the range of the rear mirror M_2 along the opposite direction of the incident or reflected light, and to find the value of the mirror coordinates of the rear mirror M_2.

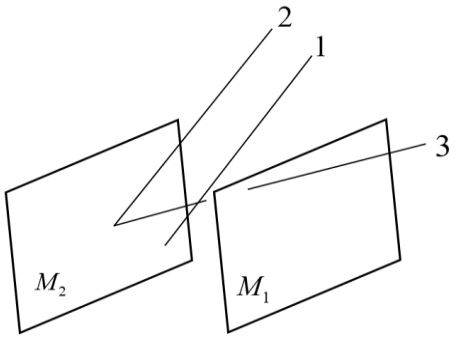

Figure 5. Schematic diagram of shadow masking simulation

Fig 5, 1, 2 for the incident light, 3 for the reflected light reflected by the mirror, by the light path can be seen, the incident light 1 in the process of incident to the M_2 mirror coincidentally blocked by the M_1 mirror, so that the M_1 mirror in the M_2 mirror to produce a shadow. And the light 2 reflected by M_2 mirror reflected light 3 to reach the collector in the process of M_2 mirror blocking caused by M_2 mirror on M_1 mirror shading phenomenon.

Let a line of incident light (or reflected light) be a vector in the ground coordinate system $\overrightarrow{V_0}$:

$$\overrightarrow{V_0} = (a, b, c), \tag{6}$$

Calculate the shadow masking loss, i.e., according to the point $H_1 = (x_1, y_1)$ on the coordinate system of the target mirror M_2, find the point $H_2 = (x_2, y_2)$ on the coordinate system of the masking mirror M_1 and judge whether H_2 falls into the mirror or not. The unit matrix of the transformation relationship from the specular coordinate system to the ground coordinate system is shown in equation (7).

$$T = \begin{pmatrix} l_x & l_y & l_z \\ m_x & m_y & m_z \\ n_x & n_y & n_z \end{pmatrix}, \tag{7}$$

where the vectors of the 3 axes of the mirror coordinate system in the ground coordinate system are (l_x, m_x, n_x) , (l_y, m_y, n_y) , (l_z, m_z, n_z) .

The coordinate system transformation equations are different for different heliostat tracking methods. Based on the traditional heliostat, the coordinate system transformation equation is shown in equation (8).

$$T = \begin{pmatrix} l_x & l_y & l_z \\ m_x & m_y & m_z \\ n_x & n_y & n_z \end{pmatrix} = \begin{pmatrix} -\sin E_H & -\sin A_H \cos E_H & \cos A_H \cos E_H \\ \cos E_H & -\sin A_H \cos E_H & \cos A_H \sin E_H \\ 0 & \cos A_H & \sin A_H \end{pmatrix}, \tag{8}$$

Where $A_H = \arctan\left(\dfrac{\cos\alpha_s \sin\gamma_s - \dfrac{h}{\sqrt{x^2+y^2+(H-h)^2}}}{\cos\alpha \sin\beta - \dfrac{x}{\sqrt{x^2+y^2+(H-h)^2}}}\right)$ is the azimuth angle of the mirror and $E_H = \arccos\left(\dfrac{\sin\alpha + \dfrac{h}{\sqrt{x^2+y^2+(H-h)^2}}}{\left|\vec{R}-\vec{I}\right|}\right)$ is the pitch angle of the mirror.

A ray of light in the mirror coordinate system is denoted by the vector $\overrightarrow{V_H}$,in the ground coordinate system is denoted by the vector $\overrightarrow{V_0}$,then there exists a transformation equation in the form of equation (9).

$$\overrightarrow{V_0} = \begin{pmatrix} l_x & l_y & l_z \\ m_x & m_y & m_z \\ n_x & n_y & n_z \end{pmatrix} \cdot \overrightarrow{V_H}, \tag{9}$$

Summarizing the above analysis, the steps for solving H_2 are as follows:

(1) Converts H_1 to H_1' in the ground coordinate system.

$$H_1' = \begin{pmatrix} l_x & l_y & l_z \\ m_x & m_y & m_z \\ n_x & n_y & n_z \end{pmatrix} \cdot H_1 + O_A = \begin{pmatrix} x_1' \\ y_1' \\ z_1' \end{pmatrix}, \tag{10}$$

where $O_A = \left(x_{M_1}, y_{M_1}, z_{M_1}\right)$ is the coordinate value of the origin of the M_1 mirror coordinate system in the ground coordinate system.

(2) Convert H_1' to H_1'' in the M_2 mirror coordinate system.

$$H_1'' = \begin{pmatrix} l_x & l_y & l_z \\ m_x & m_y & m_z \\ n_x & n_y & n_z \end{pmatrix}^T \cdot \left(H_1' - O_B\right) = \begin{pmatrix} x_1'' \\ y_1'' \\ z_1'' \end{pmatrix}, \tag{11}$$

(3) where $O_B = \left(x_{M_2}, y_{M_2}, z_{M_2}\right)$ is the coordinate value of the origin of the M2 mirror coordinate system in the ground coordinate system.

(4) Converts $\overrightarrow{V_0}$ to a vector $\overrightarrow{V_H}$ in the mirror coordinate system.

$$\overrightarrow{V_H} = \begin{pmatrix} l_x & l_y & l_z \\ m_x & m_y & m_z \\ n_x & n_y & n_z \end{pmatrix}^T \cdot \overrightarrow{V_0} = (a,b,c), \tag{12}$$

(5) Calculate the point of intersection of the ray with the M2 mirror in the M2 mirror coordinate system.

(6) According to the principle that two points determine a straight line, under the M2 mirror coordinate system $H_1'' = \left(x_1'', y_1'', z_1''\right)$, $\overrightarrow{V_H} = (a, b, c)$, solve for $H_2 = (x_2, y_2, 0)$ according to equation (13).

$$\frac{x_2 - x_1''}{a} = \frac{y_2 - y_1''}{b} = \frac{-z_1''}{c} \tag{13}$$

Solving for it yields that

$$\begin{cases} x_2 = \dfrac{cx_1'' - az_1''}{c} \\ y_2 = \dfrac{cy_1'' - bz_1''}{c} \end{cases}, \tag{14}$$

Determine whether H_2 is in the mirror coordinate system, since this question defines the width and height of the heliostat to be 6m, you only need to determine whether the absolute value of x_2 and y_2 is less than 3. If the value is less than 3, then it will be blocked, and vice versa.

The average value of different moments on 21st day of each month was taken as the monthly average shadow occlusion efficiency of that month and the data was obtained with the help of MATLAB as in Table 3.

Table 3 Average shadow occlusion efficiency on 21st day of each month

Date	Average truncation efficiency	Date	Average shadow occlusion efficiency
1.21	0.7540	7.21	0.9485
2.21	0.7152	8.21	0.8831
3.21	0.7855	9.21	0.7785
4.21	0.8875	10.21	0.7156
5.21	0.9482	11.21	0.7596
6.21	0.9612	12.21	0.7849

3.4. Cut-off efficiency

Due to the mirror's surface error, tracking error, light scattering, solar shape error and other factors, the sunlight reflected by the mirror can not all be received by the collector, which leads to part of the energy loss, called the truncation efficiency. Generally, there are two methods to find the truncation efficiency: the ray tracing method and the energy flow density method.

There exists the formula $\overrightarrow{S_s} = (\sin\sigma\cos\tau, \sin\sigma\sin\tau, \cos\sigma)$ in the ray tracing method, in which the angle between any light ray in the light cone and the main light ray from the center of the sun σ and x axis τ cannot be solved [10]. And because through the study of the distribution of the light energy, we get that the light energy distribution obeys the Gaussian distribution, and we get the expression of the truncation efficiency as Eq. (15).

$$\eta_i = \frac{1}{2\pi\sigma_{tot}^2} \iint_{xy} \exp\left(-\frac{x^2 + y^2}{2\sigma_{tot}^2}\right) dxdy , \tag{15}$$

where σ_{tot} is the overall error.

$$\sigma_{tot} = \left(\sigma_{sunshape}^2 + \sigma_{mirror}^2 + \left(2 \cdot \sigma_{track}\right)^2\right), \tag{16}$$

Where, $\sigma_{sunshape} = 2.09$ is the dispersion of sunlight with the same RMS, because the heliostat is a plane mirror and there is no refraction in the plane mirror, so the mirror dispersion of the surface error distribution of the heliostat $\sigma_{mirror} = 0$, $\sigma_{track} = 0.94$ is the tracking error of the heliostat.

The average of different moments on 21st of each month is taken as the monthly average truncation efficiency for that month and the data is obtained with the help of MATLAB as shown in Table 4.

Table 4 Average truncation efficiency on the 21st day of each month

Date	Average truncation efficiency	Date	Average truncation efficiency
1.21	0.7418	7.21	0.7418
2.21	0.7418	8.21	0.7418
3.21	0.7418	9.21	0.7418
4.21	0.7418	10.21	0.7418
5.21	0.7418	11.21	0.7418
6.21	0.7418	12.21	0.7418

4. Results

4.1. Output thermal power of a fixed-heaven mirror field

The expression for the optical efficiency of the heliostat is given in equation (17).

$$\eta=\eta_{sb}\eta_{\cos}\eta_{at}\eta_{trunc}\eta_{ref}\ , \tag{17}$$

Where $\eta_{sb}=1-\text{Shadow occlusion loss}$, $\eta_{trunc}=\frac{\text{The collector receives energy}}{\text{Specular reflection-Shading loses energy}}$ is the collector cut-off efficiency and $\eta_{ref}=0.92$ is the specular reflectance.

The expression for the output thermal power of the fixed-heaven mirror field is given in Eq. (18).

$$E_{field}=DNI\cdot\sum_{i}^{N}A_i\eta_i\ , \tag{18}$$

Where $DNI=G_0\left[a+b\exp\left(-\frac{c}{\sin\alpha_s}\right)\right]$. $a=0.4237-0.00821\left(6-H\right)^2$

$b=0.5055+0.00595\left(6.5-H\right)^2$, $c=0.2711+0.01858\left(2.5-H\right)^2$, $G_0=1.366\,\text{kW/m}^2$ is the solar constant and H is the altitude.

Combining the above analyses, the relevant data were obtained as in Tables 5 and 6.

Table 5 Question 1 average optical efficiency and output power on the 21st day of each month

Date	Average optical efficiency	Average cosine efficiency	Average shadow occlusion efficiency	Average truncation efficiency	Average output thermal power per unit area mirror (Kw/m^2)
1.21	0.3575	0.7199	0.7540	0.7418	0.3592
2.21	0.3488	0.7404	0.7152	0.7418	0.3893
3.21	0.3938	0.7611	0.7855	0.7418	0.4109
4.21	0.4556	0.7793	0.8875	0.7418	0.4252
5.21	0.4930	0.7893	0.9482	0.7418	0.4318
6.21	0.5017	0.7924	0.9612	0.7418	0.4336
7.21	0.4931	0.7892	0.9485	0.7418	0.4317
8.21	0.4529	0.7786	0.8831	0.7418	0.4248
9.21	0.3898	0.7601	0.7785	0.7418	0.4100
10.21	0.3478	0.7378	0.7156	0.7418	0.3861
11.21	0.3593	0.7182	0.7596	0.7418	0.3561
12.21	0.3676	0.7111	0.7849	0.7418	0.3422

Table 6 Problem 1-year average optical efficiency and output power

Annual average optical efficiency	Annual average cosine efficiency	Annual average shadow occlusion efficiency	Annual average truncation efficiency	Annual average output thermal power (MW)	Average output thermal power per unit area mirror (kW/m^2)
0.4134	0.7565	0.8268	0.7418	25.13	0.4001

5. Conclusions

In this paper, the annual average cosine efficiency of the heliostat field is 0.7565 according to the different pitch angles and azimuth angles of the heliostat, and the ground coordinate system and the mirror field coordinate system are converted to each other cleverly, and the average shading efficiency is 0.8268 by using the multiple ray tracing method, and the annual average truncation efficiency is 0.7418 by using the energy flow density method, and the air transmittance is 0.9652, specular reflectance is 0.92, the annual average optical efficiency is 0.4134, and the annual average output thermal power of the heliostat mirror field is 25.13 MW, which gives a better assessment of the performance of the heliostat mirror field.

In this paper, the selection of the number of light rays of the ray tracing method may be small and there is a certain error, as well as the selection of special points of the heliostat mirror there is a certain error, if the number of light rays of the selection of the performance of the heliostat mirror field in the future will be studied to get a relatively more accurate results.

References

[1] Lei Xiandao, Shuai Qifeng, Zhang Zhuoqun, et al. The principle of tower solar thermal power generation system[J]. Hydropower and new energy, 2023(12): 10-13.

[2] Xinyu Wang, Lan Li, Minghuan Guo, Zhifeng Wang, Xigang Li, Xiliang Zhang. Tracking practice of azimuth-pitch dual-axis tracking heliostat[J]. Journal of Solar Energy, 2020, 41(11): 8.

[3] Liu Jiaying Design of a tower solar heliostat tracking and control system [D]. North Central University, 2023.

[4] Wei Xiudong,Lu Zhenwu,Lin Zi,et al. Optimized design of mirror field for tower solar thermal power plant [J]. Journal of Optics, 2010, 30(09): 2652-2656.

[5] Guo Minghuan. Comparison of dual axis tracking and concentrating methods for heliostat mirrors [R]. Beijing: National Solar Thermal Alliance, 2018.

[6] P. Zhang, Z. Xi, Z. Stability, W. Han Hua, J. Wang, D. Sun. Calculation method of optical efficiency of solar tower photothermal mirror field [J]. Technology and Market, 2021, 28(6): 5-8.

[7] Liu Jianxing. Modeling simulation of optical efficiency and optimal arrangement of heliostat mirror field for tower-type photovoltaic power plant [D]. Lanzhou: Lanzhou Jiaotong University, 2022.

[8] Rui Wu. Analysis and simulation study of tower-type solar thermal power generation fixed-sun mirror system [D]. Beijing: North China Electric Power University, 2020.

[9] Feng Jieqing, Yuan Xuejiao, Zhao Yuhong. Calculation method for shadow and occlusion efficiency of tower solar mirror field CN202010449600.1[P] 2024.

[10] Du Yuhang, Liu Xiangmin, Wang Xingping, Jiang Zhihao. Impact analysis of different focusing strategies of heliostats in tower-type photovoltaic power plants[J]. Journal of Power Engineering, 2020, 40(5): 426-432